Vestibular defects in head-tilt mice result from mutations in *Nox3*, encoding an NADPH oxidase

Rainer Paffenholz,[1] Rebecca A. Bergstrom,[2] Francesca Pasutto,[1] Philipp Wabnitz,[1] Robert J. Munroe,[2] Wolfgang Jagla,[1] Ulrich Heinzmann,[3] Andreas Marquardt,[1] Armin Bareiss,[1] Jürgen Laufs,[1] Andreas Russ,[4] Gabriele Stumm,[1] John C. Schimenti,[2] and David E. Bergstrom[2,5]

[1]Ingenium Pharmaceuticals AG, D-82152 Martinsried, Germany; [2]The Jackson Laboratory, Bar Harbor, Maine 04609 USA; [3]GSF-National Research Center for Environmental Health, Institute of Pathology, 85764, Germany; [4]Genetics Unit, Department of Biochemistry, University of Oxford, Oxford OX1 3QU, UK

The vestibular system of the inner ear is responsible for the perception of motion and gravity. Key elements of this organ are otoconia, tiny biomineral particles in the utricle and the saccule. In response to gravity or linear acceleration, otoconia deflect the stereocilia of the hair cells, thus transducing kinetic movements into sensorineural action potentials. Here, we present an allelic series of mutations at the otoconia-deficient head tilt (*het*) locus, affecting the gene for NADPH oxidase 3 (*Nox3*). This series of mutations identifies for the first time a protein with a clear enzymatic function as indispensable for otoconia morphogenesis.

Received November 26, 2003; revised version accepted February 2, 2004.

The mammalian inner ear consists of the cochlea, adapted for the sensation of sound; and the vestibular system, adapted for sensation of balance, orientation, and acceleration. Within the vestibular system, the three semicircular canals and their associated sensory structures, the cristae ampullares, act in concert to detect angular acceleration. Within the saccule and utricle of the vestibular system, the neuroepithelial maculae detect gravity and linear acceleration. Above the maculae, embedded in a layer of acellular matrix, lie the otoconia, crystalline structures that act as inertial masses subject to the effects of gravity and shifting in response to linear acceleration. It is the movement of these otoconia that stimulates macular hair cells to generate action potentials that are transmitted to the brain.

Otoconia are comprised of proteinaceous and inorganic components. In mammals, the inorganic component that provides the mass and gives the otoconia their crystalline structure is primarily calcium carbonate. In addition, many of the protein components of the otoconia/matrix complex in mice are known. For example, otoconin 90 (*Oc90*) is the major protein component of otoconia with sequence (but most likely not functional) homology to phospholipase A2 (Wang et al. 1998, 1999). Otogelin (*Otog*) is a protein expressed by supporting cells and localized to the acellular membranes surrounding the otoconial crystals (Cohen-Salmon et al. 1997; El-Amraoui et al. 2001). Otoancorin (*Otoa*) is a protein localized at the interface of the sensory cells and the overlying acellular structures (Zwaenepoel et al. 2002). Despite this structural knowledge, the mechanisms of otoconial synthesis at the molecular level remain unclear.

To further understanding of balance and gravity perception, investigators have relied on the molecular genetic analysis of mice harboring mutations that specifically affect the vestibular system. Three classical loci are known that confer congenital and specific absence of otoconia in affected mice. Tilted-head (*thd*) is a classical locus mapping to mouse Chromosome 1 (Chr 1; Kelly and Hartman 1958). It has not been characterized molecularly, and to the best of our knowledge is now extinct. A second locus, tilted (*tlt*), resides on mouse Chr 5 and was recently identified as otopetrin 1 (*Otop1*; Ornitz et al. 1998; Ying et al. 1999; Hurle et al. 2001, 2003). In the present Communication, we describe the cloning and characterization of head tilt (*het*), a third locus, residing on Chr 17 (Sweet 1980; Bergstrom et al. 1998; Cook 1999).

Mice with the head tilt (*het*) mutation are characterized by impaired otoconial morphogenesis with normal functionality of the auditory system. Here we present an allelic series of mutations at the *het* locus (including three novel, mutagenesis-induced alleles), affecting the gene for NADPH oxidase 3 (*Nox3*). This series of mutations identifies for the first time a protein with a clear enzymatic function as indispensable for otoconial morphogenesis, and leads to a new model for the formation of otoconia.

Results and Discussion

In the course of our recessive ENU mutagenesis screen at Ingenium (Russ et al. 2002; Stumm et al. 2002) and our ES-cell EMS mutagenesis screen at The Jackson Laboratory (Munroe et al. 2000), animals from three independent lines (designated R96, R542, and *vst*) were identified with balance defects. These mice were characterized by an abnormally "tilted" position of the head (Fig. 1A) and abnormal performance in several motor coordination tests. The traits showed Mendelian recessive inheritance.

Balance problems among homozygous mutant mice from all three lines were most obvious when animals were held by the tail and dropped onto a soft surface from a height of 30 cm. Whereas wild-type animals always land on their feet, homozygous mutants fall on their backs or on their sides. Performance among affected mice was also severely reduced in several other tests, including stationary beam, postural reflexes, and coat

[*Keywords*: Mouse; vestibular system; otoconia; NADPH oxidase; saccule; utricle]
[5]Corresponding author.
E-MAIL deb@jax.org; FAX (207) 288-6078.
Article published online ahead of print. Article and publication date are at http://www.genesdev.org/cgi/doi/10.1101/gad.1172504.

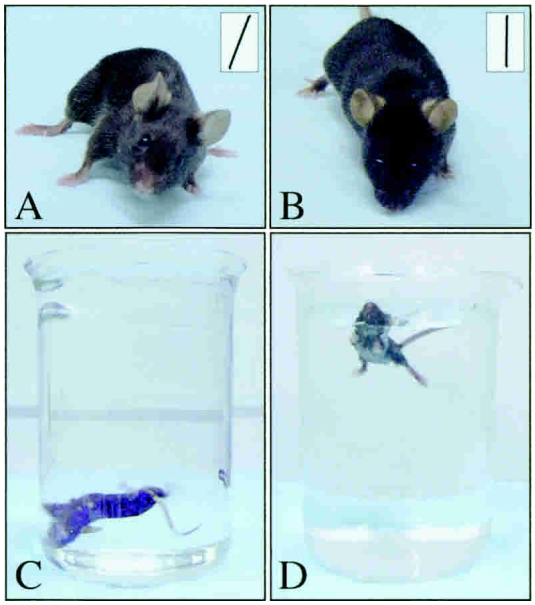

Figure 1. Typical features of R96, R542, and *vst* mutant mice. (*A*) Tilted position of the head (affected mouse). (*B*) Unaffected control. In both *A* and *B*, the angle of the head is shown in the *inset*. (*C*) Unable to swim or float in forced swim test (affected mouse). (*D*) Unaffected control.

hanger (Lalonde and Strazielle 1999). In particular, when tested in the Porsolt forced swim test (Porsolt 1979), affected mice were unable to swim or float but instead "rotated" under water and had to be taken out of the basin after a few seconds to prevent drowning (Fig. 1C). Audiometric tests of hearing ability showed normal function of the auditory system in affected and wild-type littermates from all lines (data not shown).

A histological analysis of inner ear morphology revealed the complete lack of otoconia in both the utricle and saccule of affected mice in all embryonic stages examined, starting at embryonic day 14 (E14), as well as in inner ears of newborn and adult mice (Fig. 2). In heterozygotes, the number and structure of otoconia appear to be normal. Besides the lack of the otoconia, the morphology of all other structures of the inner ear, including the sensory epithelium, is not altered in homozygous mutant mice. Because mammals use otoconia to sense their orientation in space and to monitor posture and movements, the behavior and motor coordination deficits of the three lines can be conclusively explained by the lack of otoconia.

Mice of the spontaneous mutant mouse line head-tilt (*het*; Sweet 1980) and a second allele (het^{2J}; Cook 1999) are known to have a very similar phenotype, including the complete lack of otoconia (Bergstrom et al. 1998). To test for possible allelism, homozygotes for *het* and each of the R96, R542, and *vst* lines were intercrossed. All compound heterozygotes showed the characteristic mutant phenotype, indicating that the R96, R542, and *vst* mutations each represent novel alleles at the *het* locus. We have renamed our newly identified *het* alleles het^{R96}, het^{R542}, and het^{3J}, respectively.

Head-tilt was previously mapped on Chr 17 to cM position 4.1. To fine-map the mutation in line het^{R96}, homozygous animals (strain C3HeB/FeJ) were outcrossed to C57BL/6J. The resulting F1 hybrids were intercrossed to produce a total of 375 F2 offspring, 26% of which exhibited the *het* phenotype. Analysis of recombinant animals with microsatellite markers localized het^{R96} to a critical interval between *D17Ing4* and the centromere. Phenotypically positive F2 offspring from an outcross of line het^{R542} were used to map the critical interval to an overlapping region on Chr 17 defined by the centromere and the marker *D17Ing9*. In a parallel approach, the classical *het* mutation was mapped using an overlapping series of Chr 17 deletions (You et al. 1997; Bergstrom et al. 1998, 2003) to a smaller interval between *D17Brg18* and *D17Brg198* on mouse Chr 17.

To narrow the region even further, a BAC clone (RP23-27N1) from the region (Fig. 3A), was retrofitted with neomycin and used to transfect embryonic stem (ES) cells.

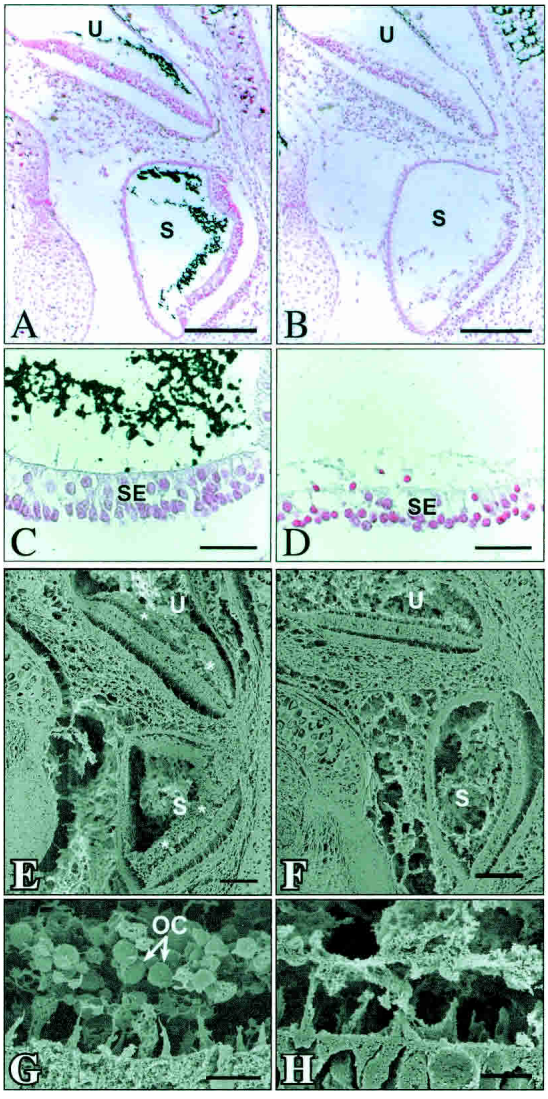

Figure 2. (*A–D*) *Kossa*-staining of inner ear transversal sections. The utricle (U) and saccule (S) of +/+ animals (*A*,*C*) contain dark stained, *Kossa*-positive otoconia, which are absent in $Nox3^{-}/Nox3^{-}$ mutant animals (*B*,*D*). (*E–H*) SEM view of transversely cut inner ear. The otoconia of the utricle (U) and saccule (S) are present in +/+ animals only (indicated by asterisks in *E*, labeled OC in *G*). In contrast, $Nox3^{-}/Nox3^{-}$ mutant animals (*F*,*H*) are devoid of otoconia. Bars: *A*,*B*,*E*,*F*, 100 µm; *C*,*D*,*G*,*H*, 10 µm.

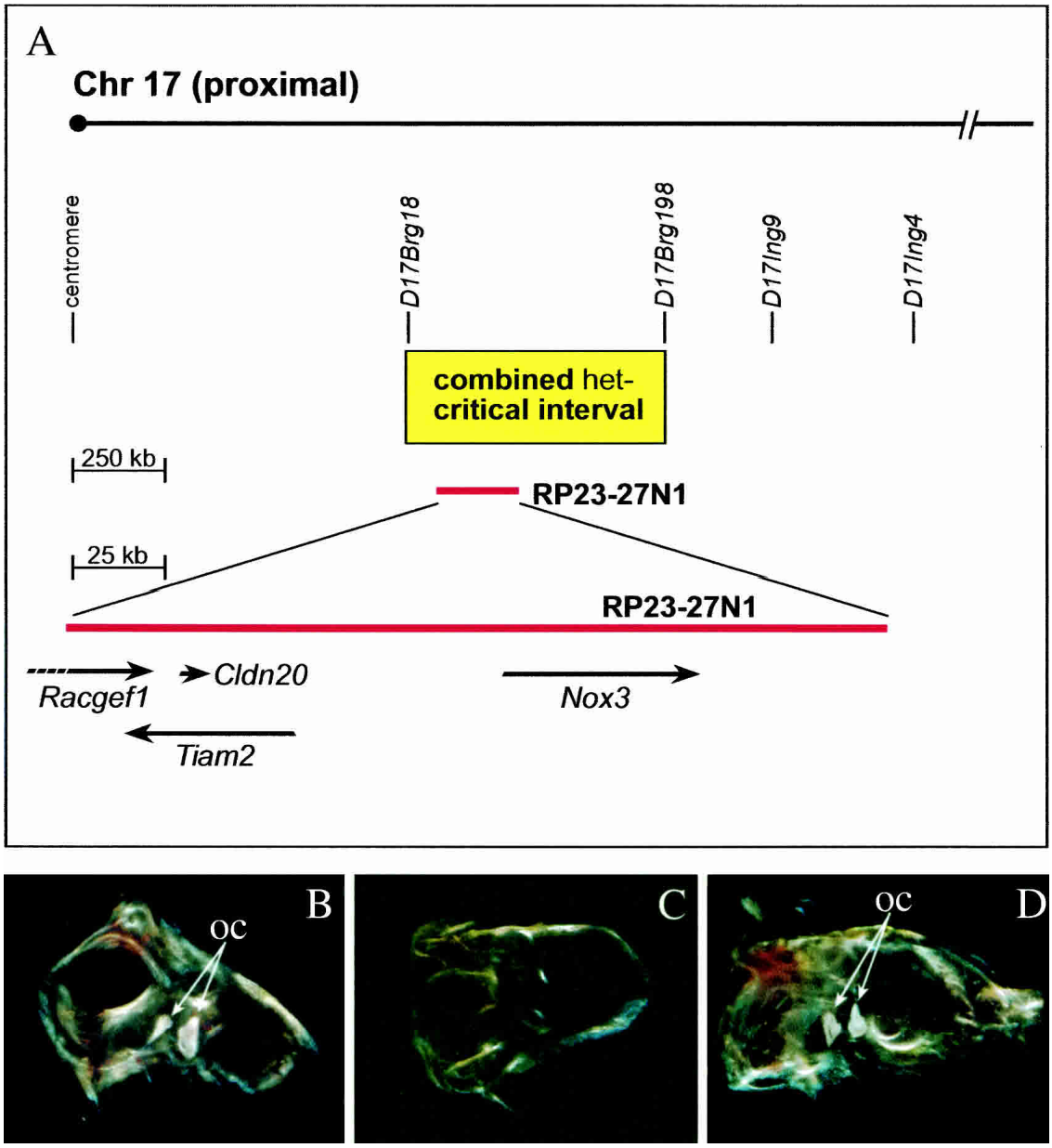

Figure 3. BAC transgenic rescue of the *Nox3* mutant phenotype. (*A*, *top*) Proximal Chr 17 showing the relative positions of significant SSLP markers, the *het*-critical region, and the rescuing BAC RP23-27N1. (*Bottom*) Enlarged view of RP23-27N1 showing the relative positions of candidate genes *Racgef1*, *Tiam2*, and *Cldn20* and the causative gene *Nox3*. (*B*) Inner ear explant from a wild-type C57BL/6J mouse showing normal otoconia. (*C*) Inner ear explant from a C57BL/6J-*het/het* mouse showing complete absence of otoconia. (*D*) Inner ear explant from a *het/het*; TgN(RP23-27N1)/+ mouse showing complete rescue/restoration of otoconia.

Transferring the BAC transgene onto the *het/het* background demonstrated that the transgene was capable of fully rescuing the mutant phenotype (Fig. 3B–D), thus limiting the critical region to the region spanned by the BAC.

Within this region, several candidate genes were identified by analysis of the mouse genomic sequence and the human syntenic region on 6q25.1. Sequencing of several candidate genes, including *Tiam2*, *Racgef1*, and *Cldn20* revealed no mutations. However, mutations were discovered in a gene highly homologous to human NADPH oxidase 3 (*NOX3*; Kikuchi et al. 2000; Cheng et al. 2001). The corresponding mouse cDNA (*Nox3*, accession no. AY182377) was PCR-amplified from embryonic (E13.5) RNA with primers deduced from the genomic sequence. It encodes a cDNA of at least 1796 nucleotides with an open reading frame of 588 codons. Identity to human *NOX3* (accession no. NM_015718) is 80% on both the cDNA and amino acid levels as determined by BLASTn and BLASTp, respectively.

In line het^{R96}, we identified a nonsense mutation at nucleotide position 441 (TA**T** → TA**A**), encoding a premature translational stop. The predicted truncated protein consists of only three transmembrane domains and lacks most of the functionally relevant features of NADPH oxidases, including the binding sites for

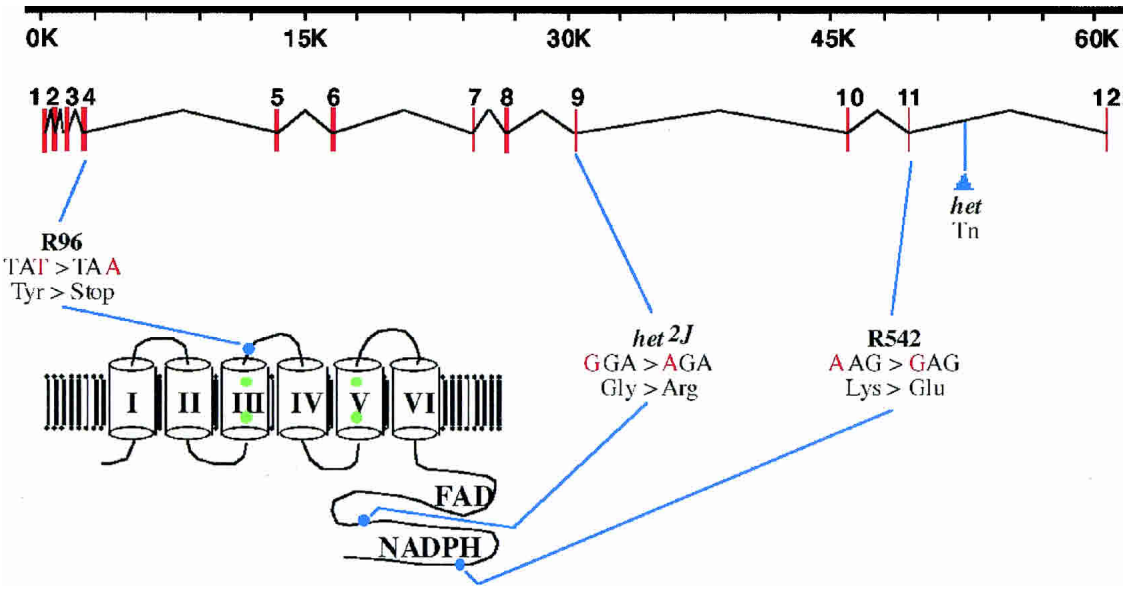

Figure 4. Genomic and amino acid structure of *Nox3*. The *top* portion of the figure shows the intron/exon structure of *Nox3*; the *lower left* portion shows the protein structure (model according to Wallach and Segal 1997). The location and nature of the R96, R542, *het*, and het^{2J} mutations are also shown.

NADPH and FAD, two of the four histidine residues presumably involved in heme binding, as well as the entire catalytic domain (Fig. 4). For Nox2 (also known as $gp91^{phox}$) and Nox5, two proteins closely related to Nox3, a proton channel function has been reported (Banfi et al. 2001; Henderson 2001). With only three transmembrane domains remaining, a similar function for the truncated Nox3 of het^{R96} can be excluded. We conclude that the *Nox3* allele of het^{R96} is a true functional null allele.

Sequencing of the *Nox3* cDNA from het^{R542} showed a nucleotide exchange at position 1576 (**A**AG → **G**AG), replacing a lysine residue with a glutamic acid. The lysine is part of a putative NADPH binding site (Cheng et al. 2001). Sequence analysis of *Nox3* from line het^{2J} revealed a nucleotide exchange at position 1282 (**G**GA → **A**GA), replacing a glycine residue with an arginine residue. This altered glycine residue is highly conserved among NADPH oxidases and is part of an NADPH binding site. RACE analysis of the classical *het* allele identified a retroviral insertion in intron 12 of the *Nox3* gene. Several mutant transcripts showing aberrant splicing from *Nox3* sequences into the retroviral element were recovered. To date, no mutation has yet been identified in the het^{3J} allele. Phenotypically, no overt differences have been observed among the five mutant alleles.

Using RT–PCR we were able to detect transcripts of the *Nox3* gene in mouse embryonic tissue as early as E10 and persisting until birth (Fig. 5). *Nox3* expression was also detected by RT–PCR analysis of mouse adult inner ear explants (Fig. 5). We could not identify mouse *Nox3* transcripts by Northern blot, multiple tissue RNA dot blot, or RNA in situ hybridization, nor could we identify Nox3 protein by Western blot or immunohistochemistry, most likely due to the low level of expression. Thus, the expression of *Nox3* in mouse resembles the results found for the human *NOX3* that has been reported to be restricted almost exclusively to embryonic tissues. As in mice, expression levels in humans are too low to be detected by Northern blotting (Cheng et al. 2001).

NADPH-oxidases are a family of proteins that generate superoxide and other reactive oxygen species (ROS). Apart from the view that ROS are simply cytotoxic byproducts of cellular metabolism, evidence has grown that Nox-generated ROS are signaling molecules in several pathways, including signaling by hormones, growth factors, and cytokines (for review, see Lambeth 2002). One mechanism whereby ROS exert their signaling capacity on proteins is by oxidation of Cys residues with an extremely low (<5.4) pKα of the sulfhydryl group. This mechanism was shown to be involved in the ROS-dependent regulation of protein tyrosine phosphatases triggered by PDGF (Meng et al. 2002).

In mammals, otoconia consist of proteins and calcium carbonate in a calcite lattice. Despite intensive study, the mechanism of otoconia formation is still a matter of debate. In a recent model, the major protein of otoconia, termed otoconin 90, is secreted from the supporting cells of the nonsensory epithelium into the endolymphatic compartments whereas supporting cells of the sensory

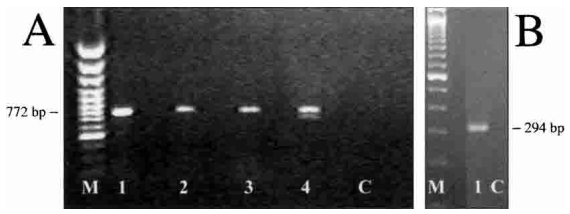

Figure 5. RT–PCR analysis of *Nox3* in different stages of mouse development. (*A*) Embryo. *Nox3* is already present by E12 and persists throughout development. (M) 100-bp marker; (1) E13.5 embryo head; (2) E13.5 without head; (3) E18.5 head; (4) E10–E12 pooled; (C) no template control. (*B*) Adult ear. *Nox3* is also present in adult ear preparations. (M) 100-bp marker; (1) adult ear; (C) no template control.

epithelium secrete numerous small vesicles ("globular substance") with a high concentration of Ca^{2+} (Thalmann et al. 2001). Although otoconin 90 and otopetrin 1, another protein recently identified to be essential for otoconia formation (Hurle et al. 2003), and the globular substance are found in the HCO_3^- enriched environment of the endolymph, the process of otoconia formation remains obscure. Interestingly, otoconin 90 has two PLA_2 (phospholipase A)-like domains with a very low pI (3.9 and 4.9), containing more than 20 Cys residues (Wang et al. 1998). In a hypothetical model, otoconin binds to the phospholipids of the globular substance vesicle membrane and undergoes a conformational change triggered by ROS produced by Nox3 located in the plasma membrane of the vesicles. This conformational change paves way for the nucleation of calcite crystal formation from the calcium provided by the vesicles and the hydrocarbonate ions of the endolymph.

Materials and methods

Audiometry

The hearing ability of het^{R96} and het^{R542} animals was tested using a startle reflex system (SR-LAB, San Diego Instruments). The mice were placed in the testing chambers with a background noise level of 70 dB. After an acclimation period of 5 min they were exposed to 60 msec white noise stimuli of 80, 90, 100, 110 and 120 dB. Each stimulus was applied 10 times with randomly placed intermissions of 5–10 sec between each stimulus. The maximum startle response during a 100 msec time frame starting with onset of each single noise stimulus was measured, and averages of the 10 stimuli with same loudness were calculated. The hearing ability of het^{2J} and het^{3J} mice was tested by startle response to a 100-dB (18.8 kHZ) sound box. *het* mice are known to have normal hearing (Jones et al. 1999).

Histology

Inner ears were obtained from fetal (E 14/16/18) and newborn +/+, +/*Nox3*$^-$, and *Nox3*$^-$/*Nox3*$^-$ mice, fixed in 4% PBS-buffered formalin, and embedded in paraffin without decalcification. After sectioning, coronal sections of both inner ears were stained with 5% silver nitrate for 30 min under strong light exposure (*von Kossa*), fixed with 5% sodium thiosulfate for 2 min, and counterstained with nuclear fast red for 3 min.

Scanning electron microscopy (SEM)

For SEM examinations the truncated tissue blocks were deparaffinized in xylene. In a graded series of ethanol the samples were dehydrated, critical-point-dried from CO_2, and sputter-coated (K575 EMITECH LTD) with 1–3-nm platinum. Coated specimens were examined in a field emission scanning electron microscope (Jeol JSM-6300F) with accelerating voltages of 5–10 kV in secondary electron mode and analyzed by an energy dispersive X-ray micro-analyzer (Link-Oxford eXL).

Positional cloning

In F2 outcross progeny, allele frequencies of C3H versus C57BL/6J are expected to be of ratio 1:1. For a marker linked to the recessive mutation, the ratio of C3H to C57BL/6J alleles is expected to increase clearly above 1. Based on this approach, we tested pooled genomic DNA from 20 affected mice on a mouse genome-wide SNP panel containing 90 polymorph markers between C3HeB/FeJ and C57BL/6J strains. This analysis resulted in linking the mutation of het^{R96} to the *Tcp10c* gene marker and the *Tap1* gene marker located in the first 18 cM of Chr 17. The result was further confirmed by a detailed haplotype analysis of all affected and nonaffected animals genotyped with the same flanking markers. To further refine the map location and narrow down the candidate region, the genomic DNA of the F2 progeny was genotyped with a series of in-house established SSLP markers covering the full candidate region and separated from each other by ~0.3 Mb. Using this approach, the critical interval was localized distal to the centromere and proximal to SSLP marker *D17Ing4* (forward PCR primer, TCCCATTTCTGATCCCTTCA; reverse PCR primer, GCAGACCGCTAGCTTAGGAA).

Similarly, the mutation in line het^{R542} was mapped to an overlapping chromosomal region distal to the centromere and proximal to SSLP marker *D17Ing9* (Fig. 4; forward PCR primer, AATTCACCCCACAAA TCCTG; reverse PCR primer, GCAGTGGTCATTGTGACAGC).

In our deletion mapping strategy, C57BL/6J-*het*/*het* mice were mated to a series of regional Chr 17 deletions (Bergstrom et al. 2003). Deletions $D17Aus9^{df\text{-}2J}$, $D17Aus9^{df\text{-}4J}$, $D17Aus9^{df\text{-}7J}$, $D17Aus9^{df\text{-}10J}$, $D17Aus9^{df\text{-}12J}$, $D17Aus9^{df\text{-}13J}$, $D17Aus9^{df\text{-}18J}$, $D17Aus9^{df\text{-}25J}$, $D17Aus9^{df\text{-}27J}$, $D17Aus9^{df\text{-}33J}$, T^{22H}, and T^{33H} failed to complement *het*. The *het* locus was complemented by $D17Aus9^{df\text{-}11J}$ and $Sod2^{df\text{-}1J}$. Detailed analysis of the deletion breakpoints in these lines with a series of in-house SSLP markers localized *het* to an interval between *D17Brg18* (forward primer, GAGGTTT TTGGCTGTAAGTGC; reverse primer, TTCACAAACTACTGACACT GCAAA) and *D17Brg198* (forward primer, ACAACAATGCCTGAGGT TGA; reverse primer, CAAAGTGGCTCACTCTCTGC).

BAC rescue

BAC RP23-27N1 was retrofitted with neomycin at the *lox*511 site using the pRetro–ES vector (Storb et al.). Following linearization with PI-SceI (New England Biolabs), the BAC was then transfected into $D17Aus9^{df\text{-}27J}$ ES cells using DOTAP transfection reagent (Roche) and the protocol supplied by the manufacturer. Neomycin-resistant clones were expanded and tested for the presence of the T7 BAC end (using the T7 primer TAATACGACTCACTATAGGG and the mouse-specific primer TGGG GAATTTTTACAGAGCCTA), the SP6 BAC end (using the SP6 primer CATACGATTTAGGTGACACTATAG and the mouse-specific primer GCCAAGGTGTAACTTGTGGA), and the vector backbone (using the *cat*-specific primers ATCCCAATGGCATCGTAAAG and GGATTGG CTGAGACGAAAAA, and *Myog*-specific internal control primers TTAC GTCCATCGTGGACAGCAT and TGGGCTGGGTGTTAGTCTTAT). ES cell clones containing both ends of the BAC were microinjected into C57BL/6J blastocysts and the resulting chimeras crossed to C57BL/6J-*het*/*het* females in the hope of placing the BAC transgene (Tg) in a $D17Aus9^{df\text{-}27J}$/*het* null background. However, due to chance and the independent assortment of the transgene and the deletion, the first transgenic pup obtained was Tg/+; +/*het*. This mouse was crossed again to C57BL/6J-*het*/*het* females and genotyped with the *het*-flanking markers *D17Brg11* (Bergstrom et al. 2003) and *D17Mit170* (Dietrich et al. 1996) to identify Tg/+; *het*/*het* males. The colony is maintained by mating these males to C57BL/6J-*het*/*het* females.

RT–PCR

To amplify partial mouse *Nox3* cDNA from embryos by PCR, primers nox3-m25F CTGGCCTGGGTATCTCTCTG (corresponding to nucleotides 587–606 of *Nox3* cDNA), and nox3-m24R CTCAGGCAGGCTCT GTGATT (nucleotides 1359–1340) were used. The primer pair produces a PCR product of 772 bp in length spanning several exon boundaries.

PCR was performed using a "touch down" method according to the following protocol: Step 1, 94°C, 5 min; Step 2, 94°C, 30 sec; Step 3, 61°C, 30 sec; Step 4, 72°C, 80 sec; two cycles; annealing temperature 59°C for two cycles; annealing temperature 57°C for two cycles; annealing temperature 55°C for 28 cycles; final extension: 10 min 72°C. PCR products were purified and sequenced.

To amplify partial mouse *Nox3* cDNA from adult inner ear preparations, primers mCG7406-37F GGCTCCCAGTGAGCTCTGTA (corresponding to nucleotides 1176–1195 of *Nox3* cDNA) and mCG7406–330R TGAGCCTTCCCTTGTTCACT (nucleotides 1469–1449) were used. The primer pair produces a PCR product of 294 bp in length spanning several exon boundaries. PCR was performed according to the following protocol: Step 1, 95°C, 120 sec; Step 2, 95°C, 45 sec; Step 3, 60°C, 45 sec; (repeating Steps 2 and 3 for 35 cycles); final extension, 7 min 72°C.

Acknowledgments

We thank the technical staff of the Ingenium R&D Group, the Ingenium Neurobiology and Pathology Group, and the Scientific Services of The Jackson Laboratory. We thank Anneliese Wunderlich, Florian Boehme, Markus Völkel, and Stephanie Kohlmann for excellent technical assistance; and Andreas Popp and Jürgen Schlegel for histopathological analysis.

This manuscript is dedicated in memory of Rebecca Bergstrom, a co-author of this work, who passed away February 6,

2004, after a lengthy battle with breast cancer. She was with us all too briefly and will be dearly missed. "Such courage, strength, and grace from such a gentle soul."

The publication costs of this article were defrayed in part by payment of page charges. This article must therefore be hereby marked "advertisement" in accordance with 18 USC section 1734 solely to indicate this fact.

References

Banfi, B., Molnar, G., Maturana, A., Steger, K., Hegedus, B., Demaurex, N., and Krause, K.H. 2001. A Ca(2+)-activated NADPH oxidase in testis, spleen, and lymph nodes. *J. Biol. Chem.* **276:** 37594–37601.

Bergstrom, R.A., You, Y., Erway, L.C., Lyon, M.F., and Schimenti, J.C. 1998. Deletion mapping of the head tilt (het) gene in mice: A vestibular mutation causing specific absence of otoliths. *Genetics* **150:** 815–822.

Bergstrom, D.E., Bergstrom, R.A., Munroe, R.J., Lee, B.K., Browning, V.L., You, Y., Eicher, E.M., and Schimenti, J.C. 2003. Overlapping deletions spanning the proximal two-thirds of the mouse t complex. *Mamm. Genome* **14:** 817–829.

Cheng, G., Cao, Z., Xu, X., van Meir, E.G., and Lambeth, J.D. 2001. Homologs of gp91phox: Cloning and tissue expression of Nox3, Nox4, and Nox5. *Gene* **269:** 131–140.

Cohen-Salmon, M., El-Amraoui, A., Leibovici, M., and Petit, C. 1997. Otogelin: A glycoprotein specific to the acellular membranes of the inner ear. *Proc. Natl. Acad. Sci.* **94:** 14450–14455.

Cook, S. 1999. The Jackson Laboratory mouse mutant resource 1999 mutation reports. In *Mouse genome informatics direct data submission.* http://www.informatics.jax.org/searches/reference.cgi?57655

Dietrich, W.F., Miller, J., Steen, R., Merchant, M.A., Damron-Boles, D., Husain, Z., Dredge, R., Daly, M.J., Ingalls, K.A., O'Conner, T.J., et al. 1996. A comprehensive genetic map of the mouse genome. *Nature* **380:** 149–152.

El-Amraoui, A., Cohen-Salmon, M., Petit, C., and Simmler, M.C. 2001. Spatiotemporal expression of otogelin in the developing and adult mouse inner ear. *Hear. Res.* **158:** 151–159.

Henderson, L.M. 2001. NADPH oxidase subunit gp91phox: A proton pathway. *Protoplasma* **217:** 37–42.

Hurle, B., Lane, K., Kenney, J., Tarantino, L.M., Bucan, M., Brownstein, B.H., and Ornitz, D.M. 2001. Physical mapping of the mouse tilted locus identifies an association between human deafness loci DFNA6/14 and vestibular system development. *Genomics* **77:** 189–199.

Hurle, B., Ignatova, E., Massironi, S.M., Mashimo, T., Rios, X., Thalmann, I., Thalmann, R., and Ornitz, D.M. 2003. Nonsyndromic vestibular disorder with otoconial agenesis in tilted/mergulhador mice caused by mutations in otopetrin 1. *Hum. Mol. Genet.* **12:** 777–789.

Jones, S.M., Erway, L.C., Bergstrom, R.A., Schimenti, J.C., and Jones, T.A. 1999. Vestibular responses to linear acceleration are absent in otoconia-deficient C57BL/6JEi-het mice. *Hear. Res.* **135:** 56–60.

Kelly, E.M. and Hartman. 1958. Tilted head, th. *Mouse News Letter* **19:** 37.

Kikuchi, H., Hikage, M., Miyashita, H., and Fukumoto, M. 2000. NADPH oxidase subunit, gp91(phox) homologue, preferentially expressed in human colon epithelial cells. *Gene* **254:** 237–243.

Lambeth, J.D. 2002. Nox/Duox family of nicotinamide adenine dinucleotide (phosphate) oxidases. *Curr. Opin. Hematol.* **9:** 11–17.

Lalonde, R. and Strazielle, C. 1999. Motor performance of spontaneous murine mutations with cerebellar atrophy. In: *Handbook of molecular-genetic techniques for brain and behaviour research* (eds. W.E. Crusio and R.T. Gerlai), pp. 627–637. Elsevier, Amsterdam.

Meng, T.C., Fukada, T., and Tonks, N.K. 2002. Reversible oxidation and inactivation of protein tyrosine phosphatases in vivo. *Mol. Cell* **9:** 387–399.

Munroe, R.J., Bergstrom, R.A., Zheng, Q.Y., Libby, B., Smith, R., John, S.W., Schimenti, K.J., Browning, V.L., and Schimenti, J.C. 2000. Mouse mutants from chemically mutagenized embryonic stem cells. *Nat. Genet.* **24:** 318–321.

Ornitz, D.M., Bohne, B.A., Thalmann, I., Harding, G.W., and Thalmann, R. 1998. Otoconial agenesis in tilted mutant mice. *Hear. Res.* **122:** 60–70.

Porsolt, R.D. 1979. Animal model of depression. *Biomedicine* **30:** 139–140.

Russ, A., Stumm, G., Augustin, M., Sedlmeier, R., Wattler, S., and Nehls, M. 2002. Random mutagenesis in the mouse as a tool in drug discovery. *Drug Discov. Today* **7:** 1175–1183.

Stumm, G., Russ, A., and Nehls, M. 2002. Deductive genomics: A functional approach to identify innovative drug targets in the postgenome era. *Am. J. Pharmacogenomics* **2:** 263–271.

Sweet, H. 1980. Head tilt. *Mouse News Letter* **63:** 19.

Thalmann, R., Ignatova, E., Kachar, B., Ornitz, D.M., and Thalmann, I. 2001. Development and maintenance of otoconia: Biochemical considerations. *Ann. NY Acad. Sci.* **942:** 162–178.

Wallach, T.M. and Segal, A.W. 1997. Analysis of glycosylation sites on gp91phox, the flavocytochrome of the NADPH oxidase, by site-directed mutagenesis and translation in vitro. *Biochem. J.* **321:** 583–585.

Wang, Y., Kowalski, P.E., Thalmann, I., Ornitz, D.M., Mager, D.L., and Thalmann, R. 1998. Otoconin-90, the mammalian otoconial matrix protein, contains two domains of homology to secretory phospholipase A2. *Proc. Natl. Acad. Sci.* **95:** 15345–15350.

Wang, Y., Thalmann, I., Thalmann, R., and Ornitz, D.M. 1999. Mapping the mouse otoconin-90 (Oc90) gene to chromosome 15. *Genomics* **58:** 214–215.

Ying, H.C., Hurle, B., Wang, Y., Bohne, B.A., Wuerffel, M.K., and Ornitz, D.M. 1999. High-resolution mapping of tlt, a mouse mutant lacking otoconia. *Mamm. Genome* **10:** 544–548.

You, Y., Bergstrom, R., Klemm, M., Lederman, B., Nelson, H., Ticknor, C., Jaenisch, R., and Schimenti, J. 1997. Chromosomal deletion complexes in mice by radiation of embryonic stem cells. *Nat. Genet.* **15:** 285–288.

Zwaenepoel, I., Mustapha, M., Leibovici, M., Verpy, E., Goodyear, R., Liu, X.Z., Nouaille, S., Nance, W.E., Kanaan, M., Avraham, K.B., et al. 2002. Otoancorin, an inner ear protein restricted to the interface between the apical surface of sensory epithelia and their overlying acellular gels, is defective in autosomal recessive deafness DFNB22. *Proc. Natl. Acad. Sci.* **99:** 6240–6245.